NASA/TM-1998-208969

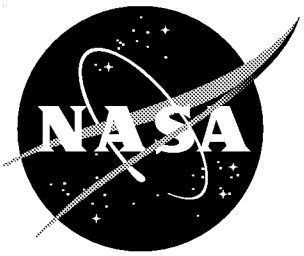

Estimation of Aircraft Nonlinear Unsteady Parameters From Wind Tunnel Data

Vladislav Klein
George Washington University
Joint Institute for Advancement of Flight Sciences
Langley Research Center, Hampton, Virginia

Patrick C. Murphy
Langley Research Center, Hampton, Virginia

December 1998

The NASA STI Program Office ... in Profile

Since its founding, NASA has been dedicated to the advancement of aeronautics and space science. The NASA Scientific and Technical Information (STI) Program Office plays a key part in helping NASA maintain this important role.

The NASA STI Program Office is operated by Langley Research Center, the lead center for NASA s scientific and technical information. The NASA STI Program Office provides access to the NASA STI Database, the largest collection of aeronautical and space science STI in the world. The Program Office is also NASA s institutional mechanism for disseminating the results of its research and development activities. These results are published by NASA in the NASA STI Report Series, which includes the following report types:

- TECHNICAL PUBLICATION. Reports of completed research or a major significant phase of research that present the results of NASA programs and include extensive data or theoretical analysis. Includes compilations of significant scientific and technical data and information deemed to be of continuing reference value. NASA counter-part of peer reviewed formal professional papers, but having less stringent limitations on manuscript length and extent of graphic presentations.

- TECHNICAL MEMORANDUM. Scientific and technical findings that are preliminary or of specialized interest, e.g., quick release reports, working papers, and bibliographies that contain minimal annotation. Does not contain extensive analysis.

- CONTRACTOR REPORT. Scientific and technical findings by NASA-sponsored contractors and grantees.

- CONFERENCE PUBLICATION. Collected papers from scientific and technical conferences, symposia, seminars, or other meetings sponsored or co-sponsored by NASA.

- SPECIAL PUBLICATION. Scientific, technical, or historical information from NASA programs, projects, and missions, often concerned with subjects having substantial public interest.

- TECHNICAL TRANSLATION. English-language translations of foreign scientific and technical material pertinent to NASA s mission.

Specialized services that complement the STI Program Office s diverse offerings include creating custom thesauri, building customized databases, organizing and publishing research results ... even providing videos.

For more information about the NASA STI Program Office, see the following:

- Access the NASA STI Program Home Page at ***http://www.sti.nasa.gov***

- E-mail your question via the Internet to help@sti.nasa.gov

- Fax your question to the NASA STI Help Desk at (301) 621-0134

- Telephone the NASA STI Help Desk at (301) 621-0390

- Write to:
  NASA STI Help Desk
  NASA Center for AeroSpace Information
  7121 Standard Drive
  Hanover, MD 21076-1320

NASA/TM-1998-208969

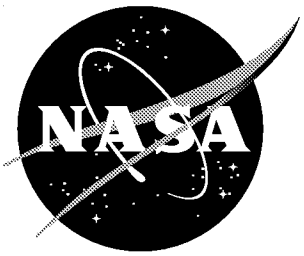

Estimation of Aircraft Nonlinear Unsteady Parameters From Wind Tunnel Data

Vladislav Klein
George Washington University
Joint Institute for Advancement of Flight Sciences
Langley Research Center, Hampton, Virginia

Patrick C. Murphy
Langley Research Center, Hampton, Virginia

National Aeronautics and
Space Administration

Langley Research Center
Hampton, Virginia 23681-2199

December 1998

Available from the following:

NASA Center for AeroSpace Information (CASI)
7121 Standard Drive
Hanover, MD 21076-1320
(301) 621-0390

National Technical Information Service (NTIS)
5285 Port Royal Road
Springfield, VA 22161-2171
(703) 487-4650

Summary

Aerodynamic equations with nonlinear unsteady effects were formulated for an aircraft in a one-degree-of-freedom large amplitude motion about each of its body axes. The corresponding aerodynamic models were expressed in the form of indicial functions. The model formulation separated the resulting aerodynamic forces and moments into static terms, purely-rotary terms and unsteady terms. For model identification from experimental data it was assumed that the static and purely-rotary terms were known. The model identification procedure developed combines a stepwise regression and maximum likelihood estimation in a two-stage optimization algorithm which can identify the unsteady term and also rotary term if necessary.

The identification scheme was applied to oscillatory data in pitch for two examples. The first example used the simulated data of a tailless aircraft, the second wind tunnel oscillatory data of the F-16XL aircraft. The results from both examples indicated that the two-stage optimization algorithm can converge to maximum likelihood estimates. The identified model from experimental data fit the data well, however, the accuracy of some of the estimated parameters was rather low, around 10%. The identified model was a good predictor for oscillatory data and data with ramp input.

Symbols

$A_j, B_j, j = 1,2,\ldots$	spline terms
$a(\alpha), b_1(\alpha)$	polynomials in α
$a_j, j = 0,1,2,\ldots$	coefficients in $a(\alpha)$
b	wing span, m
b_1	indicial function parameter, sec^{-1}
$b_{1_j}, j = 0,1,2,\ldots$	coefficients in $b_1(\alpha)$, sec^{-1}
C_a	general aerodynamic coefficient
C_L, C_m	lift and pitching-moment coefficient

$C_{a_\alpha}(t), C_{a_q}(t),$ $C_{a_\beta}(t), C_{a_p}(t),$ $C_{a_r}(t)$	indicial functions
$\bar{c}$	mean aerodynamic chord, m
$c_j, j = 0,1,\ldots,m$	coefficients in $h(t;\alpha)$
D	operator, $D = d/dt, \sec^{-1}$
$F(t;\alpha)$	model of deficiency function
$F_{a_\alpha}(t), F_{a_\beta}(t),$ $F_{a_q}(t), F_{a_\psi}(t)$	deficiency functions
$h(t;\alpha)$	sum of exponential functions, eq. (5)
k	reduced frequency, $k = \omega\ell/V$
ℓ	characteristic length, $\ell = \bar{c}/2$ or $\ell = b/2$, m
m	number of exponentials in $h(t;\alpha)$
n	number of data points
p, q, r	roll, pitch and yaw rate, rad/sec
t	time, sec
V	airspeed, m/sec
$v(i)$	measurement noise at time $(i-1)\,\Delta t$
y	variable defined by eq. (12)
z	variable defined by eq. (25)
α	angle of attack, rad or deg
β	sideslip angle, rad
Δ	increment
ε	equation error
ξ	dummy integration variable

τ	time delay, sec
ϕ	roll angle, rad
ψ	yaw angle, rad
ω	angular frequency, rad/sec

Superscript:

$\cdot$	time derivative

Subscript:

E	measured value
o	nominal value

Abbreviation:

ML	maximum likelihood
SR	stepwise regression
SNR	signal to noise ratio

Aerodynamic derivatives:

$C_{A_a}(\infty) = C_{A_a} = \frac{\partial C_A}{\partial \bar{a}}$, for $A = D, L, Y, \ell, m, \text{or } n$

for $a = p, q, r, \alpha, \dot{\alpha}, \beta \text{ or } \dot{\beta}$

and for $\bar{a} = \frac{pb}{2V}, \frac{q\bar{c}}{2V}, \frac{rb}{2V}, \alpha, \frac{\dot{\alpha}\bar{c}}{2V}, \beta, \text{ or } \frac{\dot{\beta}b}{2V}$

Introduction

One of the first attempts to obtain unsteady aerodynamic characteristics of an aircraft from experimental data was reported in reference 1. Aerodynamic models included additional state

variables to those defining aircraft motion. These additional variables were used in defining unsteady effects. Experimental data came from wind tunnel and flight tests, parameter estimation used the ordinary least squares. Further improvements to modeling and parameter estimation procedures followed and are presented in references 2 and 3. Similar approaches to model formulation and data analysis by other authors can be found in references 4 and 5.

References 6 to 8 present formulations of aerodynamic model equations in terms of indicial functions. The first of these references includes a method based on Fourier analysis of wind tunnel data from large amplitude oscillatory motion and motion generated by a ramp input. Estimation of parameters in references 7 and 8 was limited to models with linear aerodynamics. A different approach from the previous two is given in reference 9. The aerodynamic coefficients are specified as nonlinear functions of the motion variable and its rate of change. At the same time all the parameters in the model are considered as functions of frequency.

In this report, the approach of references 7 and 8 towards modeling and parameter estimation is extended to cases with nonlinear unsteady aerodynamics. After the introduction, the report presents a development of mathematical models of an aircraft performing a one degree-of-freedom motion about one of the body axes. The models developed are then used in parameter estimation with simulated and real wind tunnel data from oscillatory tests in pitch. The problem of selection or determination of a specific model structure prior to parameter estimation is also discussed. The estimation methods are based on the least squares and maximum likelihood principles. Final models are assessed as to their ability to fit the measured data and predict the aircraft motion. The report is completed by concluding remarks.

Postulated Models

In this section mathematical models of an aircraft performing a one degree-of-freedom (d.o.f.) motion about each of the three body axes will be developed. These models will be applicable to aircraft harmonic motion, response to a ramp input or any other form of a single input.

Motion in Pitch

For a one d.o.f. motion in pitch, the fundamental relations for the drag, lift and pitching moment are

$$C_a(t) = C_a\big(\alpha(t), q(t)\big), \qquad a = D, L, \text{ or } m$$

Using the results of reference 10, each of the aerodynamic coefficients can be formulated as

$$\begin{aligned} C_a(t) = C_a(0) &+ \int_0^t C_{a_\alpha}\big(t-\tau;\ \alpha(\tau), q(\tau)\big)\,\dot{\alpha}(\tau)\,d\tau \\ &+ \frac{\ell}{V}\int_0^t C_{a_q}\big(t-\tau;\ \alpha(\tau), q(\tau)\big)\,\dot{q}(\tau)\,d\tau \end{aligned} \tag{1}$$

where $C_a(0)$ is the value of the coefficient at initial steady-state conditions, $C_{a_\alpha}\big(t-\tau;\ \alpha(\tau), q(\tau)\big)$ and $C_{a_q}\big(t-\tau;\ \alpha(\tau), q(\tau)\big)$ are the indicial functions representing the change in the coefficient C_a due to the unit step in α and q respectively. The indicial responses are functions of elapsed time, $t-\tau$, and are continuous single-valued functions of $\alpha(\tau)$ and $q(\tau)$. The indicial functions approach steady-state values with increasing values of the argument $t-\tau$. To indicate this property, each indicial function can be represented as

$$C_{a_\alpha}\big(t-\tau;\ \alpha(\tau), q(\tau)\big) = C_{a_\alpha}\big(\infty;\ \alpha(\tau), q(\tau)\big) - F_{a_\alpha}\big(t-\tau;\ \alpha(\tau), q(\tau)\big)$$

and (2)

$$C_{a_q}\big(t-\tau;\ \alpha(\tau), q(\tau)\big) = C_{a_q}\big(\infty;\ \alpha(\tau), q(\tau)\big) - F_{a_q}\big(t-\tau;\ \alpha(\tau), q(\tau)\big)$$

where $C_{a_\alpha}\big(\infty;\ \alpha(\tau), q(\tau)\big)$ is the rate of change of the coefficient C_a with $\alpha(\tau)$ and $q(\tau)$, evaluated at the instantaneous value of $\alpha(\tau)$ with q fixed at the instantaneous values of $q(\tau)$. A similar definition applies for $C_{a_q}\big(\infty;\ \alpha(\tau), q(\tau)\big)$. The functions F_{a_α} and F_{a_q} are called deficiency functions.

When equations (2) are substituted in equation (1), the terms involving the steady-state parameters can be integrated and equation (1) becomes

$$C_a(t) = C_a\big(\infty;\ \alpha(t), q(t)\big) - \int_0^t F_{a_\alpha}\big(t-\tau;\ \alpha(\tau), q(\tau)\big)\ \dot{\alpha}(\tau)\ d\tau$$
$$- \frac{\ell}{V}\int_0^t F_{a_q}\big(t-\tau;\ \alpha(\tau), q(\tau)\big)\ \dot{q}(\tau)\ d\tau \qquad (3)$$

where $C_a\big(\infty;\ \alpha(t), q(t)\big)$ is the total aerodynamic coefficient that would correspond to steady flow with α and q fixed at the instantaneous values of $\alpha(t)$ and $q(t)$.

Further simplification of equation (3) can be achieved by expanding the terms in this equation in Taylor series about q = 0, taking into account only linear terms and neglecting terms in $\dot{q}$, $\dot{q}q$ and $\dot{\alpha}q$. Then

$$C_a(t) = C_a\big(\infty;\ \alpha(t), 0\big) + \frac{\ell}{V} C_{a_q}\big(\infty;\ \alpha(t), 0\big)\ q(t)$$
$$- \int_0^t F_{a_\alpha}\big(t-\tau;\ \alpha(\tau), 0\big)\ \dot{\alpha}(\tau)\ d\tau \qquad (4a)$$

or in simple notation

$$C_a(t) = C_a(\alpha) + \frac{\ell}{V} C_{a_q}(\alpha)\ q(t) - \int_0^t F_{a_\alpha}\big(t-\tau;\ \alpha(\tau)\big)\ \dot{\alpha}(\tau)\ d\tau \qquad (4b)$$

The deficiency function will be considered in the form

$$F(t;\alpha) = h(t;\alpha)a(\alpha) \qquad (5)$$

where $a(\alpha)$ is a polynomial in α, $h(t;\ \alpha)$ represents a sum of exponential functions

$$h(t;\alpha) = \sum_{j=0}^{m} c_j\ e^{-b_j(\alpha)t}$$

and $b_j(\alpha)$ are again polynomials in α. For further analysis, however, only two forms of $h(t;\alpha)$ will be considered leading to the following deficiency functions

$$F(t;\alpha) = e^{-b_1 t} a(\alpha) \qquad (6)$$

and

$$F(t;\alpha) = e^{-b_1(\alpha)t} a(\alpha) \tag{7}$$

When the differential operator, $D = d/dt$, is introduced and operator notation used, the convolution integrals with two forms of deficiency function can be expressed as

$$\int_0^t e^{-b_1(t-\tau)} a(\alpha(\tau))\dot{\alpha}(\tau)d\tau = \frac{a(\alpha)}{D + b_1} D\alpha(t) \tag{8}$$

and

$$\int_0^t e^{-b_1(\alpha(t-\tau))(t-\tau)} a(\alpha(\tau))\dot{\alpha}(\tau)d\tau = \frac{a(\alpha)}{D + b_1(\alpha)} D\alpha(t) \tag{9}$$

Incorporating equation (8) into the operational form of equation (4) and recognizing that for one d.o.f. motion in pitch $q = \dot{\alpha}$ results in

$$C_a(t) = C_a(\alpha) + \frac{\ell}{V} C_{a_q}(\alpha) D\alpha(t) - \frac{a(\alpha)}{D + b_1} D\alpha(t) \tag{10}$$

Multiplication of both sides of equation (10) by $(D + b_1)$ yields

$$\begin{aligned} DC_a(t) + b_1 C_a(t) = {} & DC_a(\alpha) + b_1 C_a(\alpha) + \frac{\ell}{V} DC_{a_q}(\alpha) D\alpha(t) \\ & + \left[\frac{b_1 \ell}{V} C_{a_q}(\alpha) - a(\alpha)\right] D\alpha(t) \end{aligned} \tag{11}$$

Equation (11) can be considered as a postulated form for model identification, i.e. for model structure determination and parameter estimation. By examining equation (11), however, it is apparent that from measured time histories $C_a(t)$, $\alpha(t)$ and their derivatives it is not possible to estimate explicitly parameter b_1 and the remaining parameters in $C_a(\alpha)$, $C_{a_q}(\alpha)$, and $a(\alpha)$. To avoid this problem, it will be further assumed that

a) $C_a(\alpha)$ is known from static measurements,

b) $C_{a_q}(\alpha)$ is estimated from small amplitude oscillatory data using techniques introduced in reference 8.

Combining time histories $C_a(t)$ with those of $C_a(\alpha)$ and $(\ell/V)\, C_{a_q}(\alpha)\, \dot{\alpha}(t)$, a new variable y can be introduced as

$$y(t) = C_a(t) - C_a(\alpha) - \frac{\ell}{V} C_{a_q}(\alpha)\, \dot{\alpha}(t) \tag{12}$$

or, by using equations (4) and (6) as

$$y(t) = -\int_0^t e^{-b_1(t-\tau)}\, a(\alpha(\tau))\, \dot{\alpha}(\tau)\, d\tau \tag{13}$$

Equation (13) in operator notation will represent Model I as

$$y(t) = -\frac{a(\alpha)}{D + b_1} D\alpha(t) \tag{14a}$$

which is equivalent to

$$\dot{y}(t) + b_1 y(t) = -a(\alpha)\, \dot{\alpha}(t) \tag{14b}$$

The second model considered incorporates dependency of the parameter b_1 on the angle of attack. Equation (13) takes more general form (see Appendix A) as

$$y(t) = -\int_0^t e^{-\int_\tau^t b_1(\alpha(\xi))\, d\xi}\, a(\alpha(\tau))\, \dot{\alpha}(\tau)\, d\tau \tag{15}$$

Model II is then defined as

$$y(t) = -\frac{a(\alpha)}{D + b_1(\alpha)} D\alpha(t) \tag{16a}$$

or

$$\dot{y}(t) + b_1(\alpha)\, y(t) = -a(\alpha)\, \dot{\alpha}(t) \tag{16b}$$

Motion in Roll and Yaw

For a one d.o.f. motion in roll at a constant value of the angle of attack, α_0, the relations for the lateral aerodynamic coefficients are

$$C_a(t) = C_a\big(\phi(t), p(t)\big); \qquad a = Y, \ell, \text{or } n$$

where the roll angle is related to the sideslip angle by the equation

$$\beta = \sin^{-1}\left(\sin\phi \sin\alpha_0\right) \tag{17}$$

The aerodynamic coefficients can be formulated as

$$\begin{aligned} C_a(t) &= C_a(0) + \int_0^t C_{a_\beta}\left(t-\tau;\ \beta(\tau), p(\tau)\right)\dot{\beta}(\tau)\, d\tau \\ &+ \frac{\ell}{V}\int_0^t C_{a_p}\left(t-\tau;\ \beta(\tau), p(\tau)\right)\dot{p}(\tau)\, d\tau \end{aligned} \tag{18}$$

If the procedure illustrated for the motion in pitch is followed, equation (18) will be simplified as

$$\begin{aligned} C_a(t) &= C_a\left(\infty;\ \beta(t), 0\right) + \frac{\ell}{V} C_{a_p}\left(\infty;\ \beta(t), 0\right) p(t) \\ &- \int_0^t F_{a_\beta}\left(t-\tau;\ \beta(\tau), 0\right)\dot{\beta}(\tau)\, d\tau \end{aligned} \tag{19}$$

where $C_a\left(\infty, \beta(t), 0\right)$ is the total aerodynamic coefficient that would correspond to steady flow at a fixed value of α and with β fixed at the instantaneous value of $\beta(t)$, and $C_{a_p}\left(\infty, \beta(t), 0\right)$ is the rate of change of the coefficient C_a with $p(t)$ evaluated at fixed value of α and instantaneous value of $\beta(t)$. F_{a_β} is the deficiency function which might take the form of equation (5).

Similarly, for a one d.o.f. motion in yaw at a constant value of α, the relations for the lateral coefficients are

$$C_a(t) = C_a\big(\psi(t), r(t)\big); \qquad a = Y, \ell \text{ or } n$$

where the yaw angle is related to the sideslip angle as

$$\beta = \sin^{-1}\left(-\sin\psi\cos\alpha_0\right) \tag{20}$$

The simplified model for the coefficients takes the form

$$C_a(t) = C_a(\beta) + \frac{\ell}{V} C_{a_r}(\beta)\, r(t) - \int_0^t F_{a_\psi}\left(t-\tau;\, \beta(\tau)\right) \dot{\psi}(\tau)\, d\tau \tag{21}$$

where the definitions of terms in (21) are similar to those for terms in equation (19).

Model Identification

Model structure determination and parameter estimation will be demonstrated on model equation (16) governing a one d.o.f. motion in pitch. Modifications to less complicated model (14) or models for a one d.o.f. motion in roll and yaw can be easily made. Substituting measured values at $t_i, i = 1,2,\ldots,n,$ into equation (16b) gives

$$\dot{y}_E(i) = -\left[b_1\left(\alpha_E(i)\right) y_E(i) + a\left(\alpha_E(i)\right) \dot{\alpha}_E(i)\right] + \varepsilon_y(i) \tag{22}$$

where index E indicates the measured values, $\varepsilon_y(i)$ is an equation error at time $(i - 1)\ \Delta t$ and Δt is the sampling interval. Equation (22) is the regression equation with the unknown parameters in polynomials $b_1(\alpha)$ and $a(\alpha)$. The mean values of these parameters can be estimated by a least squares technique. The parameter covariance matrix under the assumption of colored noise can be obtained from expressions in reference 11. In order to avoid differentiation of measured data an approach of reference 12 using modulating functions can be applied.

For estimation of parameters in equation (22) a structure of both polynomials $b_1(\alpha)$ and $a(\alpha)$ must be either known or determined from experimental data. The structure of $a(\alpha)$ can be selected from results of the small amplitude oscillatory data analysis as indicated in reference 8. If either the structure of $b_1(\alpha)$ or structures of both terms, $b_1(\alpha)$ and $a(\alpha)$, are not known, a stepwise regression can be applied to model structure determination and parameter estimation (see e.g. ref. 13).

The least squares parameter estimates can be updated by a maximum likelihood estimation method outlined in reference 11. The constraint equations are the state and measurement equations

of the form

$$\dot{y}(t) = -b_1(\alpha)\, y(t) - a(\alpha)\, \dot{\alpha}_E(t); \quad y(t=0) = y(0) \tag{23}$$

$$y_E(i) = y(i) + v(i), \quad i = 1,2,\ldots,n \tag{24}$$

where $v(i)$ is the measrement noise at time $(i - 1)\, \Delta t$.

In some cases the model for $C_{a_q}(\alpha)$ may not be known. Then the parameters in $b_1(\alpha)$ and $a(\alpha)$ will be estimated for some *a priori* values of $C_{a_q}(\alpha)$. Returning to equations (12) and (15), a new variable $z(t)$ can be formed as

$$\begin{aligned} z(t) &= C_a(t) - C_a(\alpha) + \int_0^t e^{-b_1\left(\alpha(\xi)\right) d\xi} a(\alpha)\, \dot{\alpha}(\tau)\, d\tau \\ &= \frac{\ell}{V} C_{a_q}(\alpha)\, \dot{\alpha}(t) \end{aligned} \tag{25}$$

When the measured values, and parameter estimates in $b_1(\alpha)$ and $a(\alpha)$ are substituted into (25) the regression equation is obtained as

$$z_E(i) = \frac{\ell}{V} C_{a_q}\left(\alpha_E(i)\right) \dot{\alpha}_E(i) + \varepsilon_z(i), \quad i = 1,2,\ldots,n \tag{26}$$

Based on equation (26), the model structure of $C_{a_q}(\alpha)$ can be determined and parameters in that model estimated. In the following step the parameters in $b_1(\alpha)$ and $a(\alpha)$ can be estimated again, this time for the new model of $C_{a_q}(\alpha)$ and new values of $y_E(i)$ computed from equation (12). This two-stage optimization procedure can be repeated until the minimum of the cost function for the maximum likelihood estimator is reached. A block diagram for the two-stage estimation procedure is presented in figure 1.

Examples

The procedure for identifying a nonlinear unsteady aerodynamic model of an aircraft subjected to one d.o.f. harmonic motion about one of its body axes is demonstrated in two examples. Both examples use data from pitch oscillations only. In the first example, the methodology is applied to

simulated data representing the pitching moment coefficient of a tailless aircraft. In the second example, wind tunnel data from a 10-percent-scale model of the F-16XL aircraft are used. A three-view of this model is shown in figure 2 together with some of the basic dimensions. Static and dynamic tests were conducted in the NASA Langley 12-Foot Low-Speed Wind Tunnel. A brief description of the test is given in reference 8.

Example 1

The purpose of this example is to demonstrate the feasibility of the algorithm to estimate parameters in the model with a given structure. In addition, the effect of measurement and modeling errors on the estimates will be investigated. The time histories of the pitching moment were computed from equations (4), (6) and (7), and data in table I for Model I and Model II. The expressions for $b_1(\alpha)$ and $a(\alpha)$ were postulated as splines of the form

$$a(\alpha) = a_0 + a_1\alpha + a_2\alpha^2 + \sum_{j=1}^{2} A_j\left(\alpha - \alpha_j\right)_+^2 \tag{27}$$

and

$$b_1(\alpha) = b_{10} + \sum_{j=1}^{4} B_j\left(\alpha - \alpha_j\right)_+ \tag{28}$$

where α_j are knots and $(\alpha - \alpha_j)_+$ are the plus functions defined as $(\alpha - \alpha_j)_+ = 0$, for $\alpha_j < \alpha$ and $(\alpha - \alpha_j)_+ = \alpha - \alpha_j$, for $\alpha_j \geq \alpha$.

The plots of the data in table I are presented in figure 3. Both the nominal value and amplitude of the angle of attack oscillations were selected as 35 deg, and the three frequencies of the oscillatory motion were 0.25, 0.50 and 1.00 Hz. The sampling interval was 0.01 sec. The variation of the pitching moment and its components with the angle of attack is shown in figure 4. The time histories of y and $\dot{y}$ are plotted in figure 5 for three cycles of each frequency. A zero-mean, Gaussian and white random sequence representing the measurement noise was added to the computed values of $\dot{y}$. The variance of this sequence was defined by the signal-to-noise ratio (SNR).

The effect of measurement noise on the ML estimates of b_1 and five parameters in $a(\alpha)$ is shown

in table II. The increase of noise level, SNR changed from 40 to 20, resulted in expected increase of errors in estimated parameters, and in the fit error, $s(\nu)$. The differences between parameter true and estimated values, however, remain within the 2σ-confidence intervals. In table III the effect of modeling error in b_1 is demonstrated. Replacing the spline $b_1(\alpha)$ by a constant led to a large fit error and large errors of parameters in $a(\alpha)$. The results in table III further indicate that even for correct structure of $b_1(\alpha)$, the parameters were, in general, estimated with low accuracy. Finally, in table IV the results of two-stage optimization are shown. The parameter estimation started with an incorrect model for $C_{m_q}(\alpha)$ by replacing the second-degree polynomial by a known constant. Then model structure determination and parameter estimation procedures were applied to identify a model for $C_{m_q}(\alpha)$ in regression equation (26). As indicated in table IV, after three iterations the identified model for $C_{m_q}(\alpha)$ was very close to the true one. The remaining parameter estimates were also close to their true values.

Example 2

The measured static and oscillatory data used in this example are shown in figure 6 as $C_L(\alpha)$, $C_m(\alpha)$, $C_L(\alpha; \alpha_0, \alpha_A, k)$, and $C_m(\alpha; \alpha_0, \alpha_A, k)$ where $\alpha_0 = 35$ deg, $\alpha_A = 35$ deg and $k = 0.034$, 0.057, 0.1013 and 0.1350. For the wind tunnel speed $V = 17.52$ m/sec and $\bar{c} = 0.753$ m, the corresponding frequencies were $f = 0.25$, 0.42, 0.75 and 1.00 Hz. Each of the four time histories of the oscillatory data were comprised of three cycles with the sampling rate of 100 Hz. The time histories of measured data were obtained as the average values from five repeated runs at the same amplitude and frequency. The variability of averaged data in cycles was, in general, very low. Some scatter appeared in the stall region of the pitching-moment coefficient as can be seen in figure 7, where the data from three repeated cycles are shown. The analytical forms of static data were obtained by fitting the measured $C_L(\alpha)$ and $C_m(\alpha)$ curves. For the *a priori* values of two damping terms, $C_{L_q}(\infty;\alpha)$ and $C_{m_q}(\infty;\alpha)$, the estimates from small-amplitude oscillatory data of reference 8 were used and reformulated as

$$C_{L_q}(\infty;\alpha) = -0.424 \qquad \text{for } \alpha < 20 \text{ deg}$$

$$= -2.0 + 5.7\alpha - 3.4\alpha^2 \qquad \text{for } \alpha < 20 \text{ deg}$$

and

$$C_{m_q}(\infty;\alpha) = -1.245 - 0.3806\alpha + 1.5557\alpha^2$$

The models for the polynomials $a(\alpha)$ and $b_1(\alpha)$ were postulated as polynomial splines given by equation (27) and (28) with two knots in each expression. The variable y_E was computed from equation (12), its derivative was obtained by numerical differentiation.

After two iterations of the two-stage optimization algorithm the identified models for the polynomials $a(\alpha)$ and $b_1(\alpha)$ were

$$a(\alpha) = a_1 + a_2\alpha + \sum_{j=1}^{2} A_j\left(\alpha - \alpha_j\right)_+^2 \tag{29}$$

$$b_1(\alpha) = b_0 + b_1\alpha + \sum_{j=1}^{2} B_j\left(\alpha - \alpha_j\right)_+ \tag{30}$$

for the coefficient $C_L(\alpha)$ and

$$a(\alpha) = a_0 + a_1\alpha + a_2\alpha^2 + \sum_{j=1}^{2} A_j\left(\alpha - \alpha_j\right)_+^2 \tag{31}$$

$$b_1(\alpha) = b_{10} \tag{32}$$

for the coefficient $C_m(\alpha)$.

The ML estimates of model parameters in equations (29) to (32) and their standard errors (Cramer-Rao bounds) are summarized in table V. The standard error of estimated parameters varied between 4 to 11 percent indicating possible identification problems for some parameters in the model. The plots of polynomials $a(\alpha)$ and $b_1(\alpha)$ are presented in figures 8 and 9. The *a priori* and estimated values of parameters in polynomials representing the variation of the damping terms C_{m_q} with the angle of attack are shown in table VI. The identified model had the same structure as its *a priori*

counterpart, and the accuracy of the estimated parameters was between 3 to 13 percent. As pointed out in table VI the a priori model for $C_{L_q}(\infty;\alpha)$ was not updated because of a small contribution of the C_{L_q} term to the lift. The identified final models fit the measured data very well at all frequencies. An example of measured and estimated coefficients is given in figure 10 for the reduced frequency $k = 0.057$.

The identified models were also assessed by their prediction capabilities. The predicted time histories of C_L and C_m were computed from equation (4b) for selected amplitude and frequency of the oscillatory motion or for the ramp input in the angle of attack at different rates. A comparison of measured and predicted coefficients $C_L(\alpha)$ and $C_m(\alpha)$ for two different amplitudes and similar frequencies is given in figures 11 and 12. Figures 13 and 14 present a comparison of the same coefficients for two different ramp inputs versus α. The same data in the form of time histories are shown in figures 15 and 16. The results in figures 11 to 16 indicate that the identified models are good predictors for the lift coefficient, while some discrepancies between measured and predicted data can be seen in the pitching-moment oscillatory data with the amplitude of 20 deg and the ramp data.

Concluding Remarks

Aerodynamic equations with nonlinear unsteady effects were formulated for an aircraft in a one-degree-of-freedom large amplitude motion about each of its body axes. The corresponding aerodynamic models were expressed in the from of indicial functions. The model formulation separated the resulting aerodynamic forces and moments into static terms, purely-rotary terms and unsteady terms. The unsteady term in the model for a pitching motion was modeled as a product of an exponential function and a polynomial in the angle of attack. For model identification from experimental data it was assumed that the static and purely-rotary terms were known. The model identification procedure developed combines stepwise regression and maximum likelihood estimation. In cases when the *a priori* information about the rotary term is in doubt, a two-stage optimization algorithm which can identify both the unsteady and rotary terms were proposed.

The identification scheme was applied to wind tunnel oscillatory data in pitch in two examples. The first example used the simulated data for a tailless aircraft and the second used wind tunnel oscillatory data from the F-16XL aircraft. The results from both examples indicated that

1. the two-stage optimization algorithm can converge to maximum likelihood estimates;
2. the accuracy of estimated parameters can be severely degraded by modeling errors;
3. the identified model from experimental data fit the data well, however, the accuracy of some of the estimated parameters was rather low, around 10%;
4. the identified model was a good predictor for oscillatory data and data with ramp input.

References

1. Goman, M. G.; Stolyarov, G. I.; Tyrtyshnikov, S. L.; Usolcev, S. P. and Khrabrov, A. N.: Mathematical Description of Longitudinal Aerodynamic Characteristics at High Angles of Attack Accounting for Dynamic Effects of Separated Flow. TsAGI Preprint No. 9, 1990 (in Russian).

2. Goman, M. and Khrabrov, A.: State-Space Representation of Aerodynamic Characteristics at High Angles of Attack. Journal of Aircraft, Vol. 31, No. 5, Sept.–Oct. 1994, pp. 1109–1115.

3. Goman, M.; Khrabrov, A. and Usolcev, S.: Unsteady Aerodynamic Model for Large Amplitude Maneuvers and its Parameter Identification. 11th IFAC Symposium on Identification, 8–11 July 1997, Kitakyushu, Japan, Vol. 1, pp. 399–403.

4. Fishenberg, D.: Identification of an Unsteady Aerodynamic Stall Model from Flight Test Data. AIAA Paper 95-3438-P, 1996.

5. Fan, Yigang and Lutze, Fraderick H.: Identification of an Unsteady Aerodynamic Model at High Angles of Attack. AIAA Paper 96-3407-P, 1996.

6. Chin, Suei and Lan, C. Edward: Fourier Functional Analysis for Unsteady Modeling. AIAA Paper 91-2867-P, 1991.

7. Klein, Vladislav and Noderer, Keith D.: Modeling of Aircraft Unsteady Aerodynamic Characteristics. Part 2-Parameters Estimated from Wind Tunnel Data. NASA TM 110161, 1995.

8. Klein, Vladislav; Murphy, Patrick C.; Curry, Timothy J. and Brandon, Jay M.: Analysis of Wind Tunnel Longitudinal Static and Oscillatory Data of the F-16XL Aircraft. NASA/TM-97-206276, 1997.

9. Lin, Guo-Feng and Lan, C. Edward: A Generalized Dynamic Aerodynamic Coefficient Model for Flight Dynamics Applications. AIAA Paper 97-3643, 1997.

10. Tobak, Murray and Schiff, Lewis B.: On the Formulation of the Aerodynamic Characteristics in Aircraft Dynamics. NASA TR-R-456, 1976.

11. Morelli, E. A. and Klein V.: Accuracy of Aerodynamic Model Parameters Estimated from Flight Test Data. Journal of Guidance, Control, and Dynamics, Vol. 20, No. 1 Jan.–Feb. 1997, pp. 74-80.

12. Pearson, A. E.: Aerodynamic Parameter Estimation via Fourier Modulating Function Techniques. NASA CR 4654, 1995.

13. Klein, Vladislav; Batterson, James G. and Murphy, Patrick C.: Determination of Airplane Model Structure from Flight Data by Using Modified Stepwise Regression. NASA TP 1916, 1981.

Appendix A

Integral form of Model II

The following differential equation is considered

$$\dot{y}(t) + b_1(\alpha)\, y(t) = -\, a(\alpha)\, \dot{\alpha}(t) \tag{A1}$$

where $b_1(\alpha)$ and $a(\alpha)$ are polynomials in α. After multiplying each side (A1) by the exponential term

$$e^{\int_0^t b_1(\alpha(\xi))\, d\xi}$$

and rearranging, the following relationships is obtain

$$\frac{d}{dt}\left(y(t) e^{\int_0^t b_1(\alpha(\xi))\, d\xi} \right) = -a(\alpha(t))\, \dot{\alpha}(t) e^{\int_0^t b_1(\alpha(\xi))\, d\xi} \tag{A2}$$

Integration of both sides of (A2) results in

$$y(t) e^{\int_0^t b_1(\alpha(\xi))\, d\xi} = -\int_0^t a(\alpha(\tau))\, \dot{\alpha}(\tau) e^{\int_0^\tau b_1(\alpha(\xi))\, d\xi}\, d\tau \tag{A3}$$

or

$$y(t) = -\int_0^t e^{-\left(\int_0^t b_1(\alpha(\xi))\, d\xi - \int_0^\tau b_1(\alpha(\xi))\, d\xi\right)}\, a(\alpha(\tau))\, \dot{\alpha}(\tau)\, d\tau \tag{A4}$$

Equation (A4) leads to the final form expressed as

$$y(t) = -\int_0^t e^{-\int_\tau^t b_1(\alpha(\xi))\, d\xi}\, a(\alpha(\tau))\, \dot{\alpha}(\tau)\, d\tau \tag{A5}$$

Table I. Characteristics of a tailless aircraft used in generating oscillatory data

$$C_m(\alpha) = 0.42\alpha + 0.34\alpha^2 - \alpha^3 + 0.40\alpha^4$$

$$C_{m_q}(\alpha) = -2 + 0.8\alpha^2$$

$$a(\alpha) = +0.28\alpha - 3.2\alpha^2 + 8(\alpha - 0.4363)_+^2 - 7.4(\alpha - 0.9599)_+^2$$

Model I:

$b_1 = 2.5$

Model II:

$$b_1(\alpha) = 2.5 - 5.73(\alpha - 0.349)_+ + 5.73(\alpha - 0.5236)_+ + 5.73(\alpha - 0.827)_+ - 5.73(\alpha - 1.0472)_+$$

$$\frac{\ell}{V} = 0.02131 \text{ sec}$$

Table II. Effect of measurement noise on estimated parameters. Simulated data, Model I.

Parameter	True Value	Estimate	
		SNR = 40	SNR = 20
b_1	2.5	2.503 (.0032)	2.500 (.0066)
a_1	.28	.28 (.010)	.27 (.021)
a_2	−3.2	−3.21 (.022)	−3.17 (.046)
A_1	8.0	8.0 (0.44)	7.91 (.092)
A_2	−7.4	−7.6 (.20)	−6.8 (.42)
$s(\nu)$	—	.0041	.0085

Note: numbers in parentheses are Cramer-Rao bounds on standard errors

Table III. Effect of modeling errors in $b_1(\alpha)$ on estimated parameters. Simulated data, Model II, SNR = 40.

Parameter	True Value	Estimate	
		Model II	Model I
b_{10}	2.5	2.513 (.0069)	2.277 (.0056)
B_1	−5.73	−5.9 (.12)	—
B_2	5.73	5.9 (.21)	—
B_3	5.73	5.8 (.28)	—
B_4	−5.73	−5.9 (.39)	—
a_1	.28	.26 (.013)	.67 (.021)
a_2	−3.2	−3.16 (.029)	−4.25 (.047)
A_1	8.0	7.92 (.059)	10.06 (.094)
A_2	−7.4	−7.0 (.25)	−9.2 (.43)
$s(\nu)$	—	.0045	.0087

Note: numbers in parentheses are Cramer-Rao bounds on standard errors

Table IV. Effect of modeling error in $C_{m_q}(\alpha)$ on estimated parameters. Simulated data, Model I, SNR = 40.

Parameter	True Value	Estimate	
		$C_{m_q} = -1.4$	$C_{m_q}(\alpha)$ estimated
b_1	2.5	2.385 (.0071)	2.464 (.0033)
a_1	.28	.55 (.022)	.32 (.010)
a_2	−3.2	−3.62 (.050)	−3.26 (.023)
A_1	8.0	8.49 (.099)	8.08 (.045)
A_2	−7.4	−8.1 (.45)	−7.6 (.21)
s(ν)	—	.0092	.0042

Note: a) number in parentheses are Cramer-Rao bounds on standard errors

b) initial value $C_{m_q} = -1.4$

estimate after four iterations: $C_{m_q} = -1.939 + 0.804\alpha^2$

(.0043)(.0072)

true model: $C_{m_q} = -2 + 0.8\alpha^2$

Table V. Maximum likelihood estimates of parameters in $a(\alpha)$ and $b_1(\alpha)$ polynomial splines.

Parameter	C_L	C_L knot location (degrees)	C_m	C_m knot location (degrees)
a_0	—	—	−0.52 (.054)	—
a_1	9.8 (.56)	—	5.1 (.43)	—
a_2	−31.0 (1.4)	—	−9.7 (.69)	—
A_1	50.0 (2.3)	20	18.0 (1.2)	26
A_2	−22.0 (2.5)	47.5	−11.0 (1.3)	46
b_0	12.6 (.45)	—	7.1 (.36)	—
b_1	−16.1 (.78)	—	—	—
B_1	49.0 (3.3)	45	—	—
B_2	−32.0 (4.5)	55	—	—
con	−0.14 (.018)	—	0.07 (.010)	—
$s(\nu)$	.026	—	.012	—

Note: (a) numbers in parentheses are Cramer-Rao bounds on standard errors.

(b) *con* is a constant added to the state equation.

Table VI. *A priori* values and least-squares estimates of parameters in $C_{Lq}(\infty;\alpha)$ and $C_{mq}(\infty;\alpha)$.

Parameter with	$C_{Lq}(\infty;\alpha)$		$C_{mq}(\infty;\alpha)$	
	$\alpha < 20$ deg	$\alpha > 20$ deg	*a priori*	estimated
α^0	−0.424	−2.0	−1.245	−0.97 (.027)
α	0.0	5.7	−0.381	−0.76 (.098)
α^2	0.0	−3.4	1.556	1.53 (.077)

Notes: (a) numbers in parentheses are Cramer-Rao bounds on standard errors.
(b) C_{mq} parameter estimates are obtained after two iterations.
(c) C_{Lq} was not updated due to its small contribution to C_L.

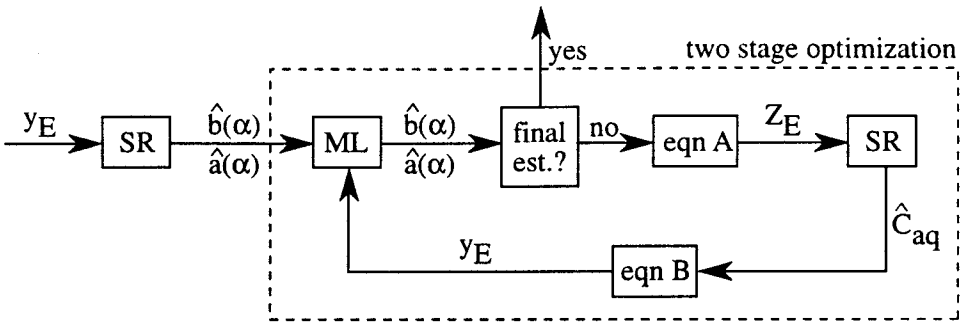

Eqn. A: $$z(t)=\left(\frac{\ell}{V}\right)C_{a_q}(\infty;\alpha,0)\,q(t)$$

Eqn. B: $$y(t)=C_a(t)-C_a(\infty;\alpha,0)-\frac{\ell}{V}C_{a_q}(\infty;\alpha,0)\,q(t)$$

Figure 1. Block diagram of model identification using stepwise regression (SR) and a maximum likelihood (ML) estimation.

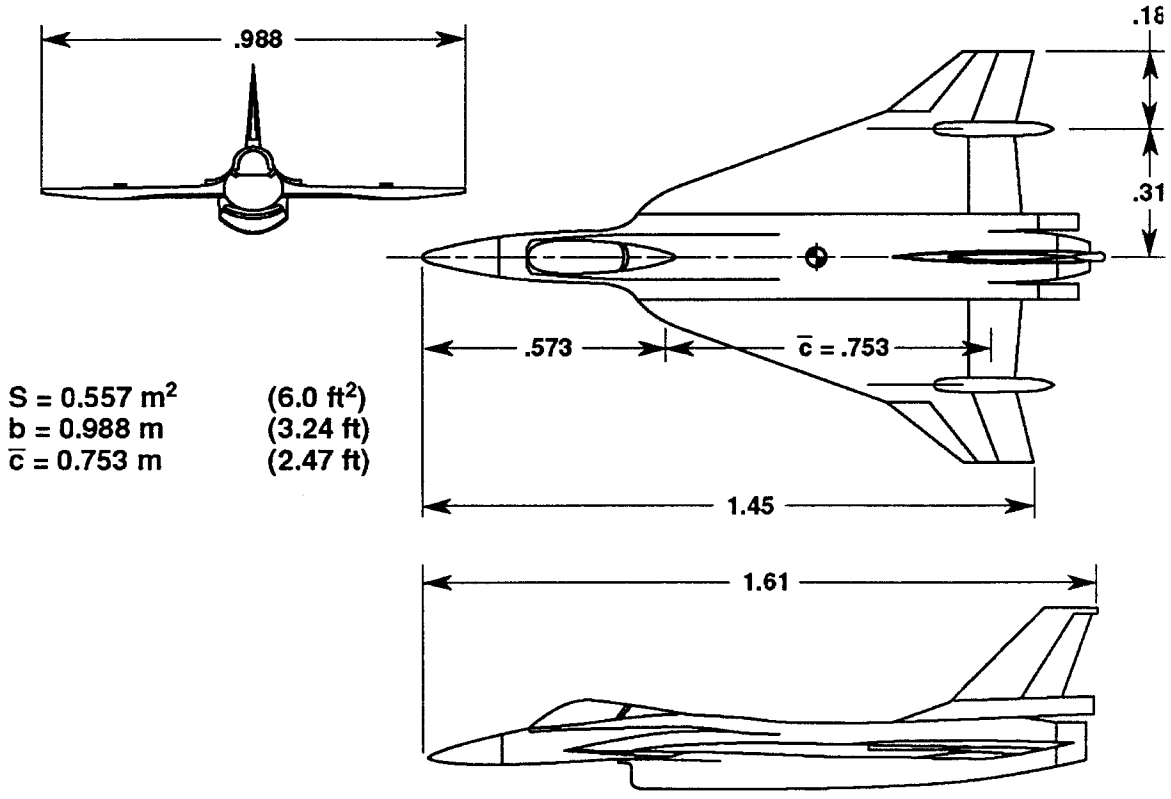

Figure 2. Three-view sketch of F-16XL model.

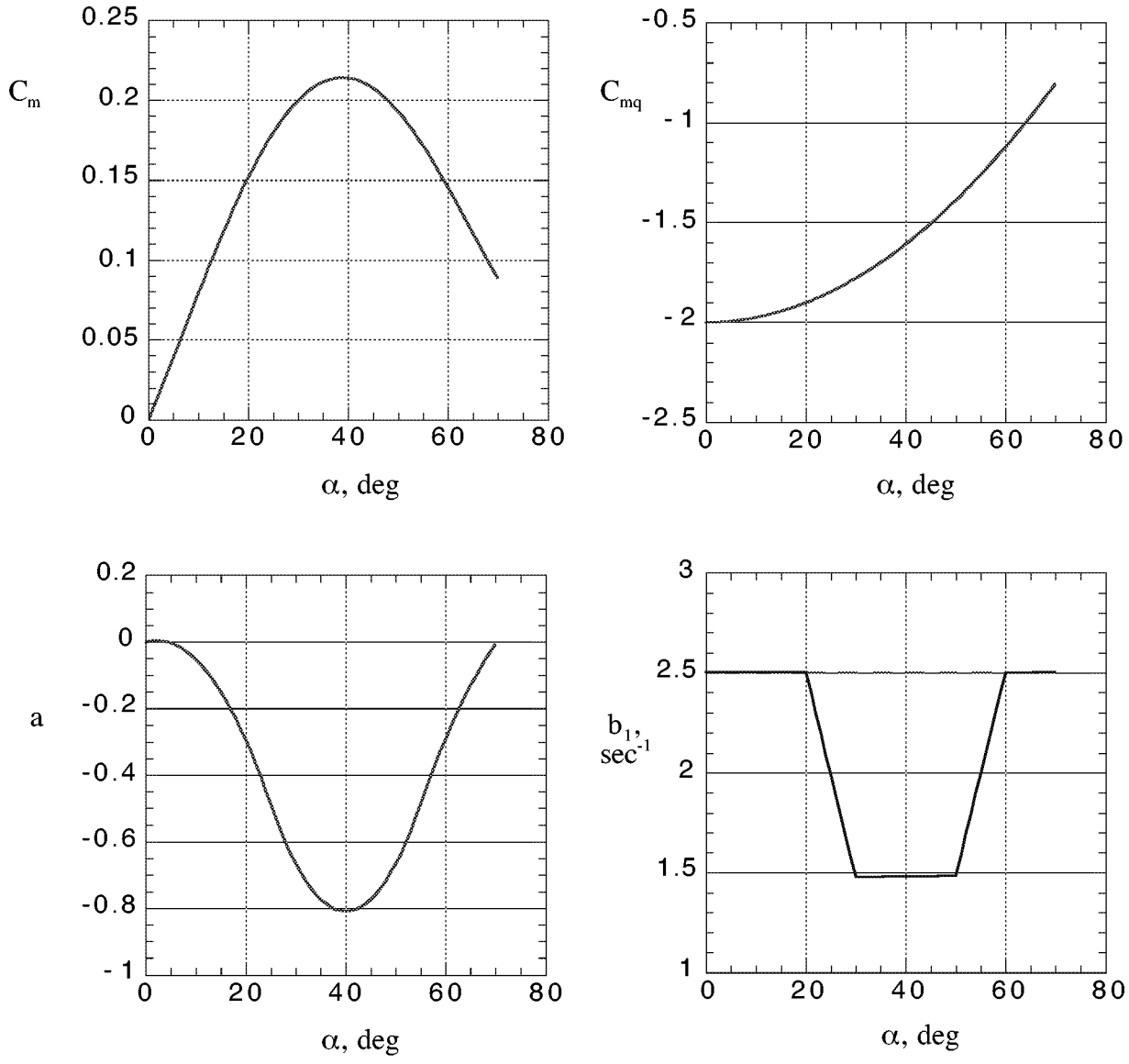

Figure 3. Aerodynamic characteristics of tailless aircraft for simulated data examples.

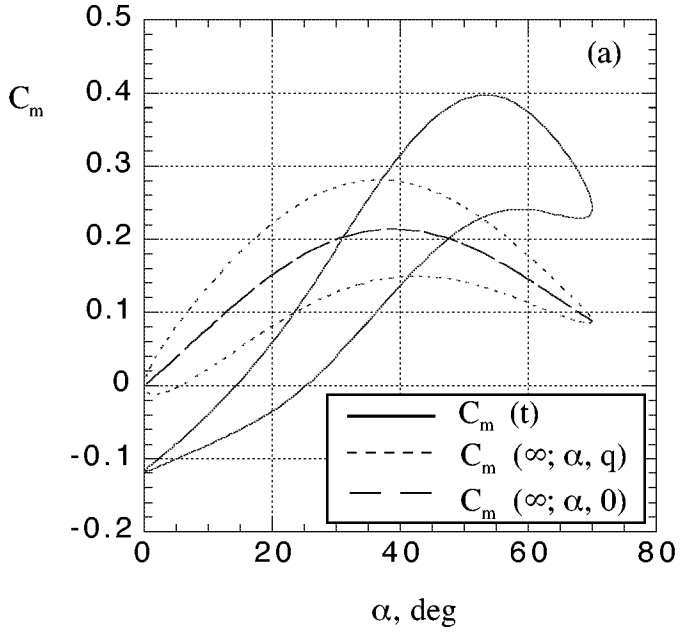

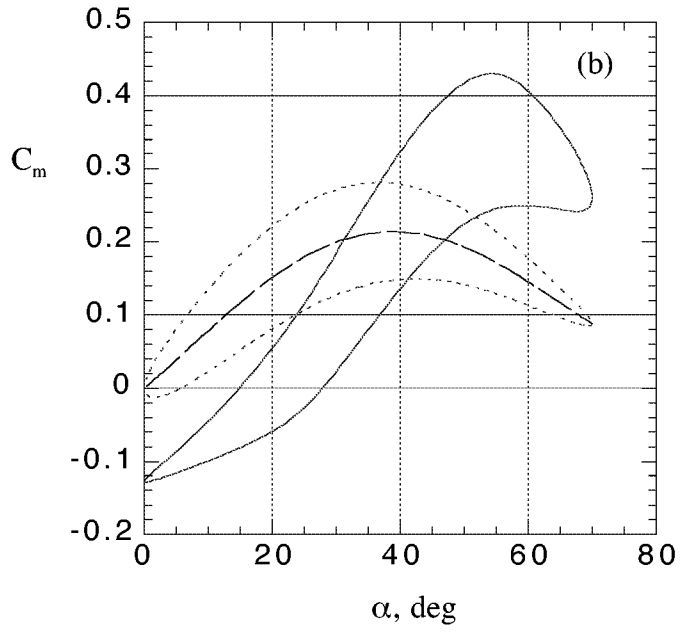

Figure 4. Pitching-moment coefficient and its components in steady oscillatory motion at $f = 0.5$ Hz. Simulated data, (a) Model I, (b) Model II.

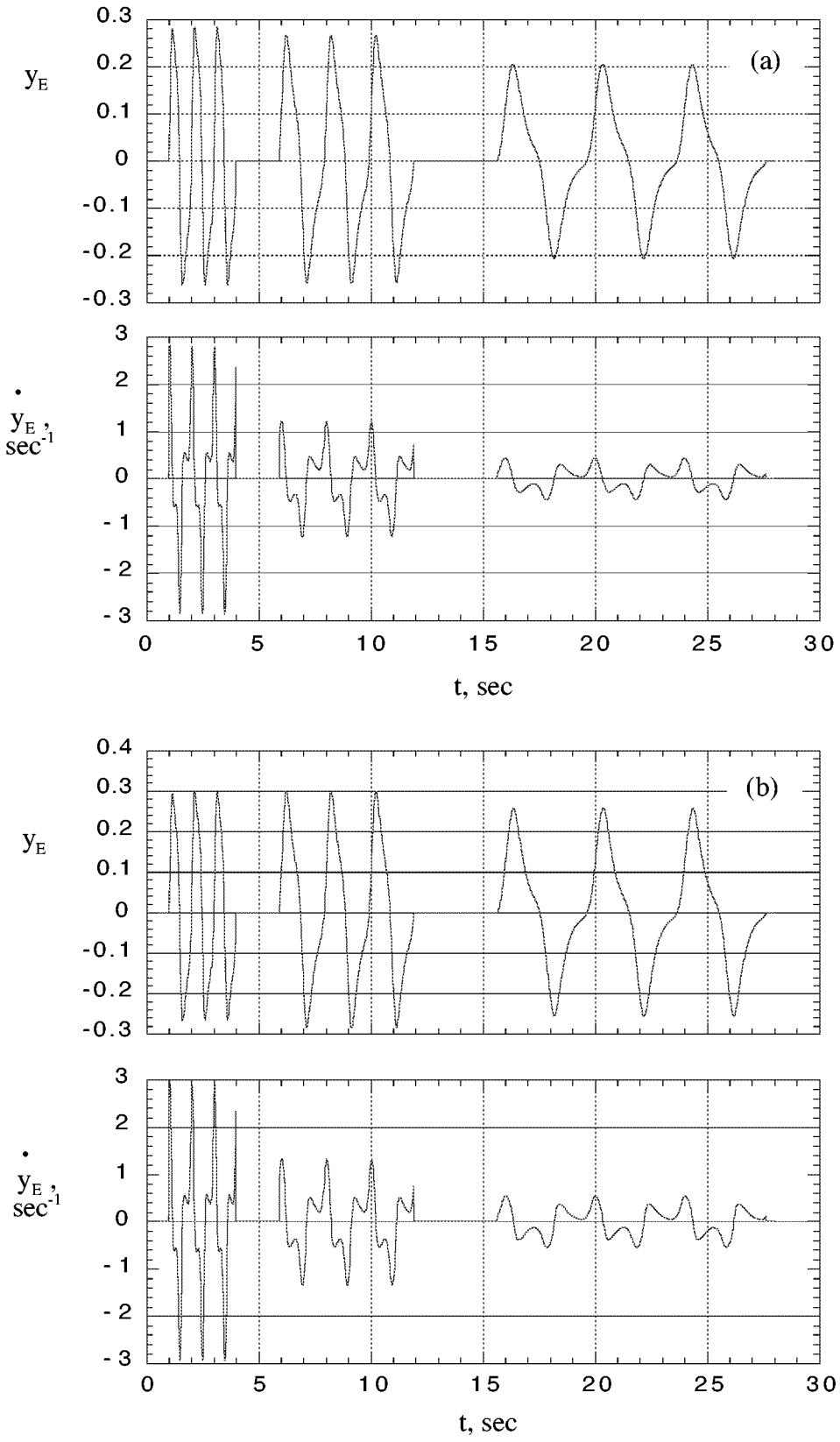

Figure 5. Time histories of dependent variable $y_E(t)$ and its derivative. Simulated data, (a) Model I, (b) Model II.

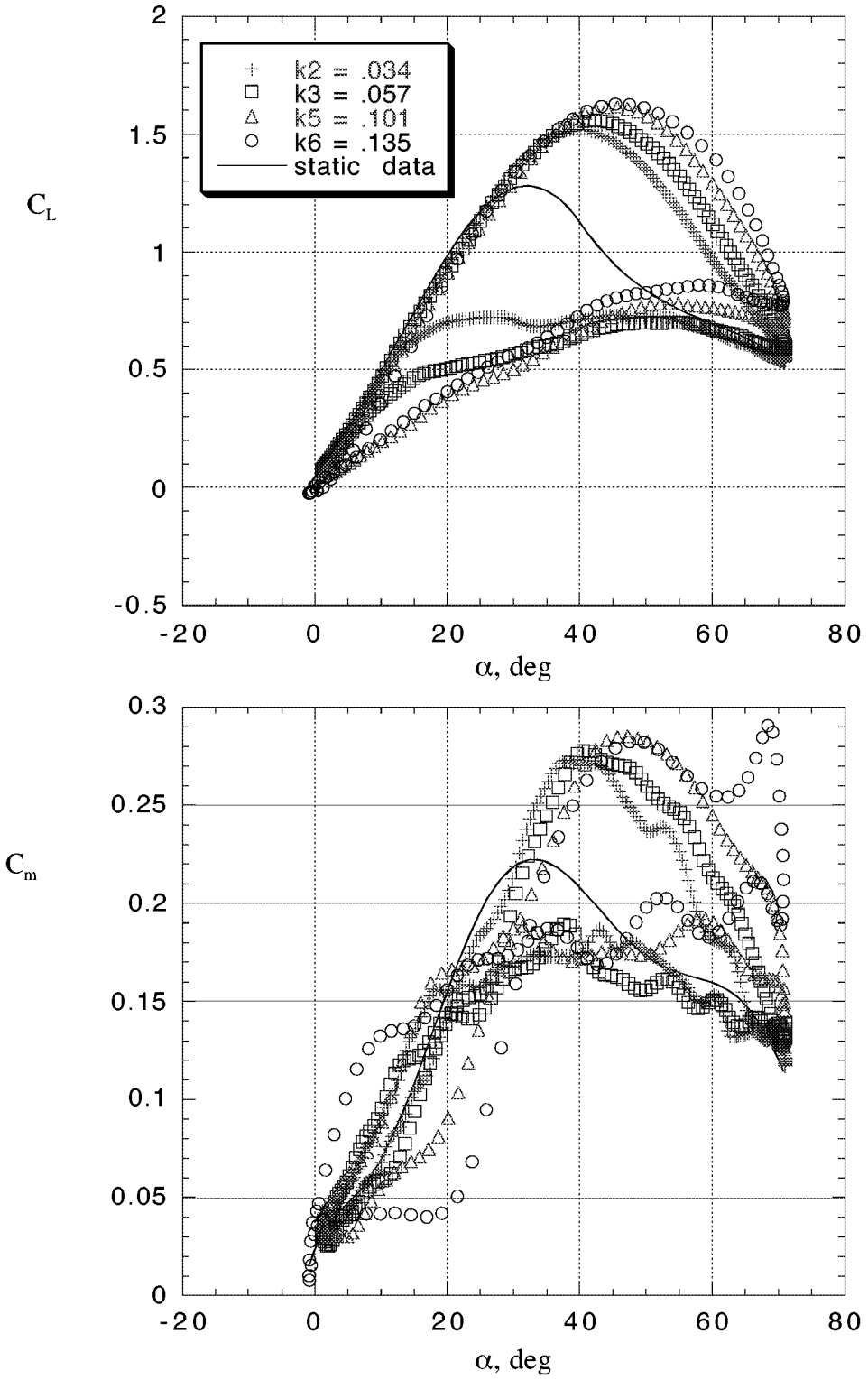

Figure 6. Wind tunnel measurements of lift and pitching moment coefficients in steady oscillatory motion at test frequencies.

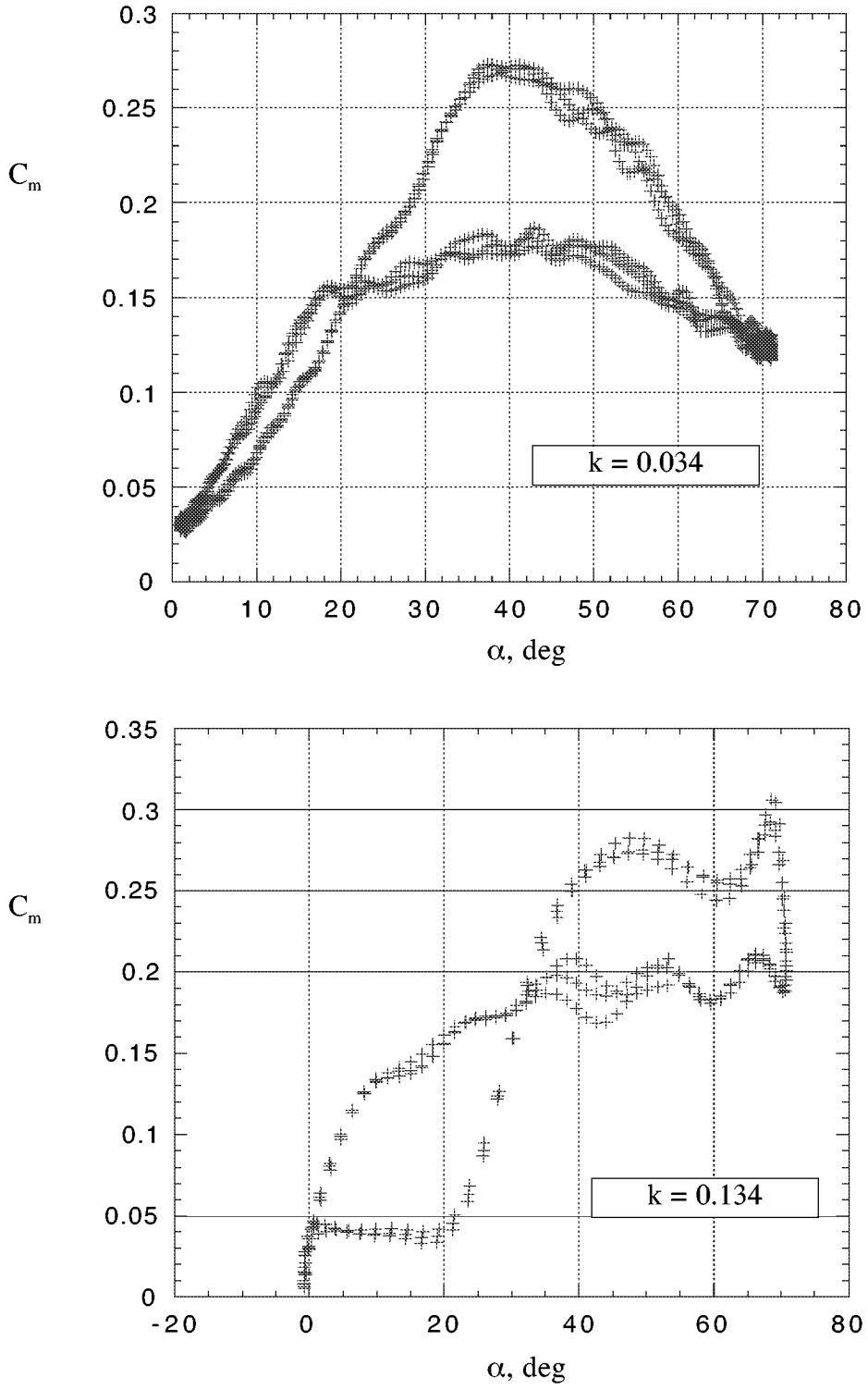

Figure 7. Data variability for wind tunnel measurements of pitching moment coefficient in steady oscillations for three cycles.

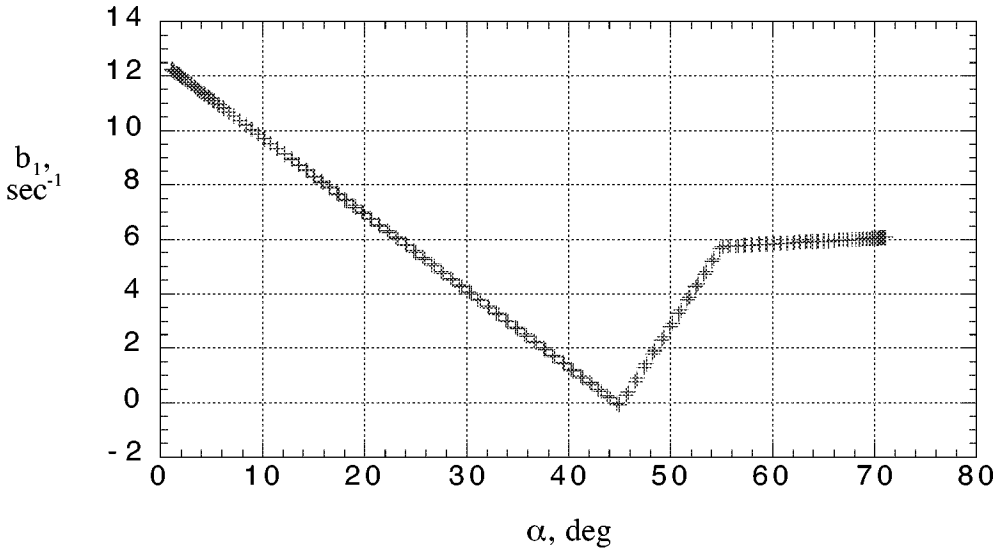

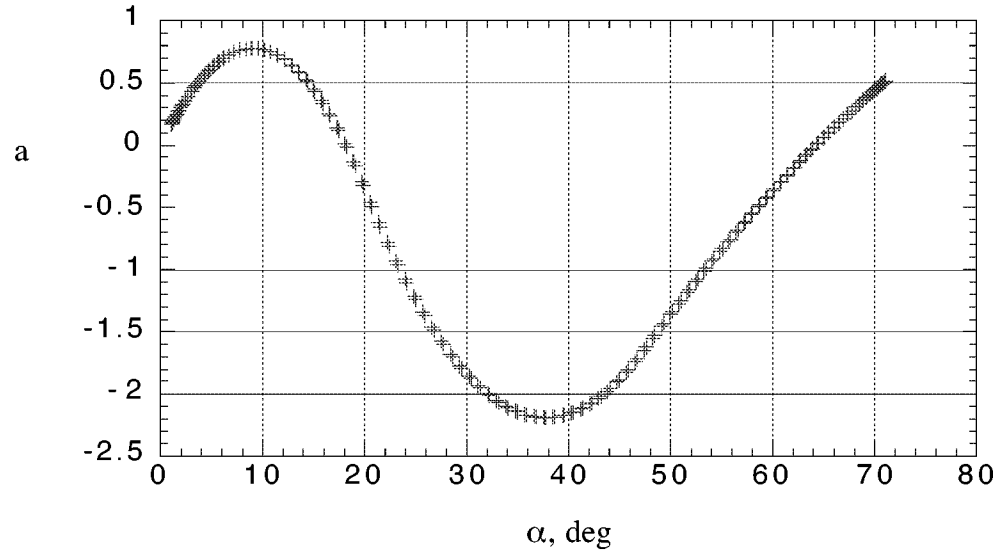

Figure 8. Estimated parameter functions for lift coefficient.

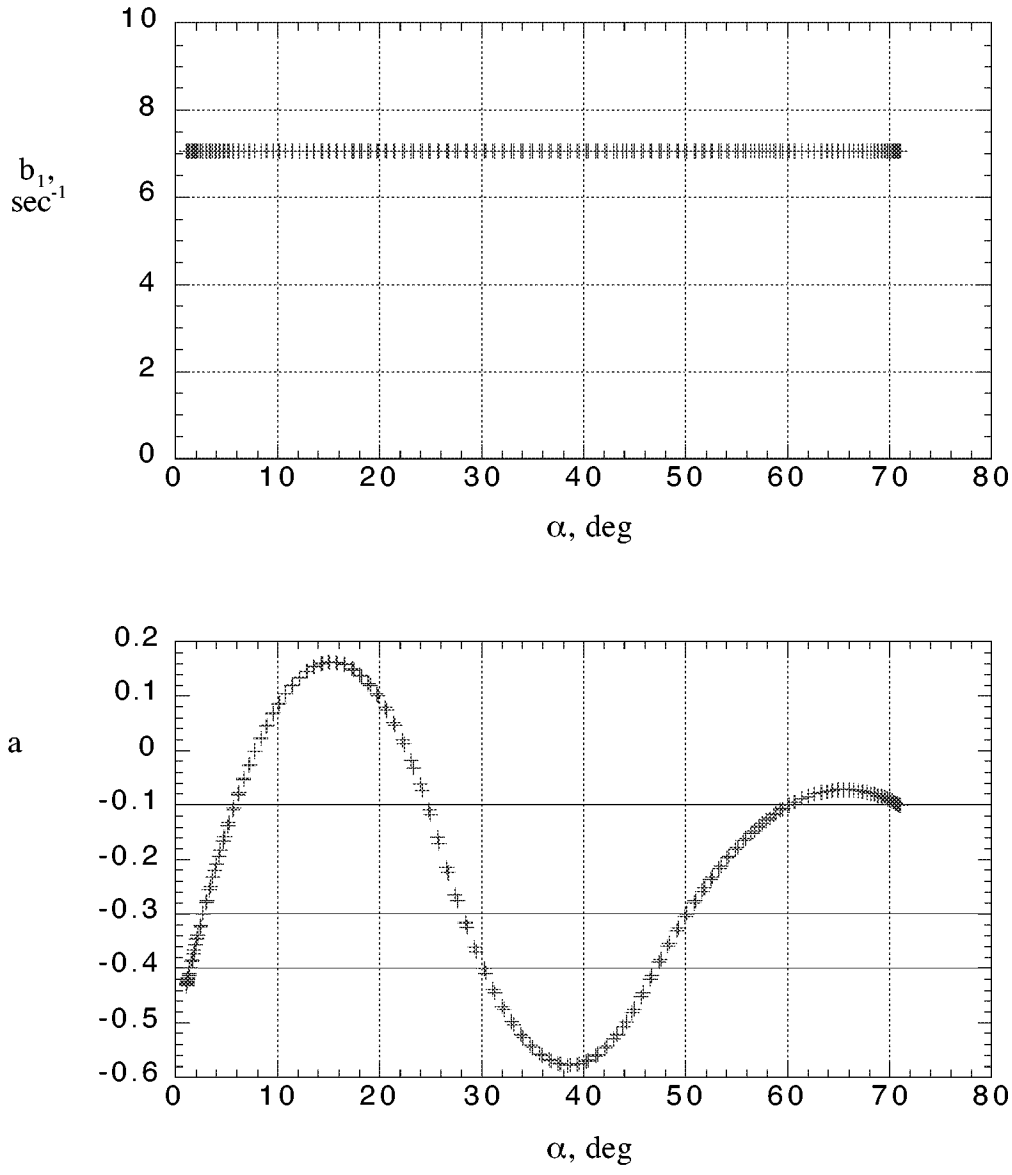

Figure 9. Estimated parameter functions for pitching moment coefficient.

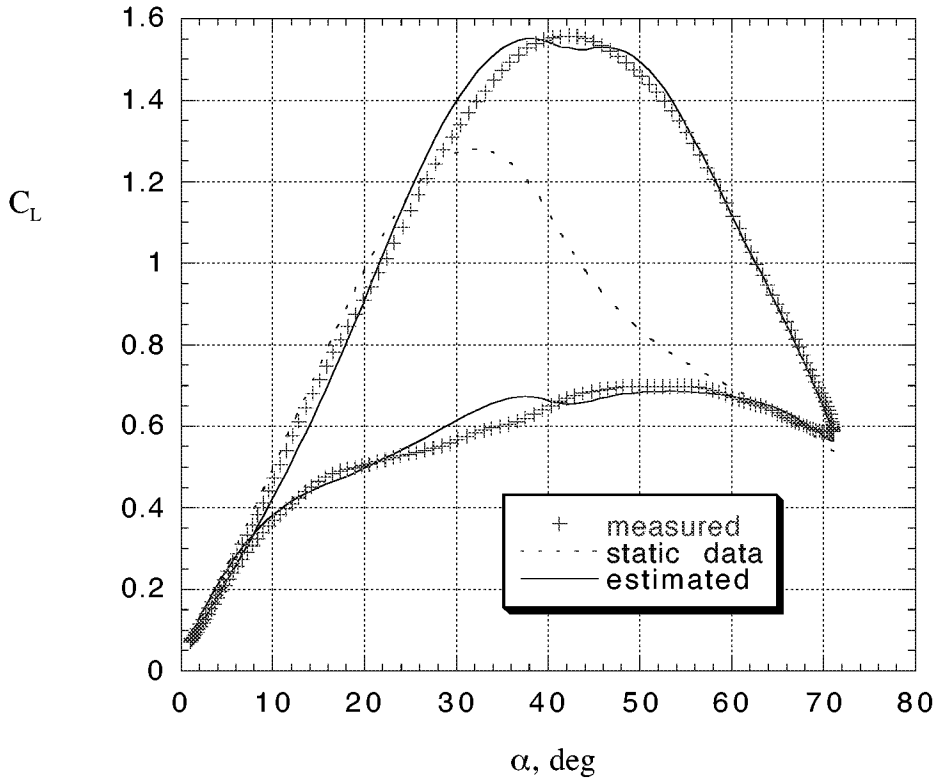

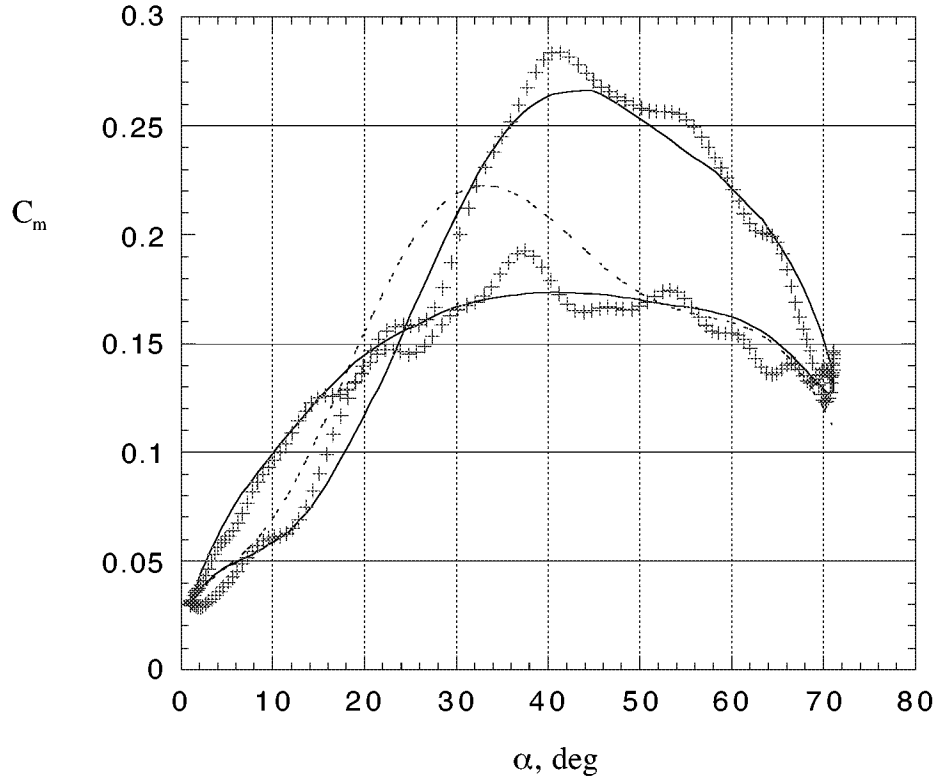

Figure 10. Measured and estimated lift and pitching-moment coefficients. $k = 0.057$.

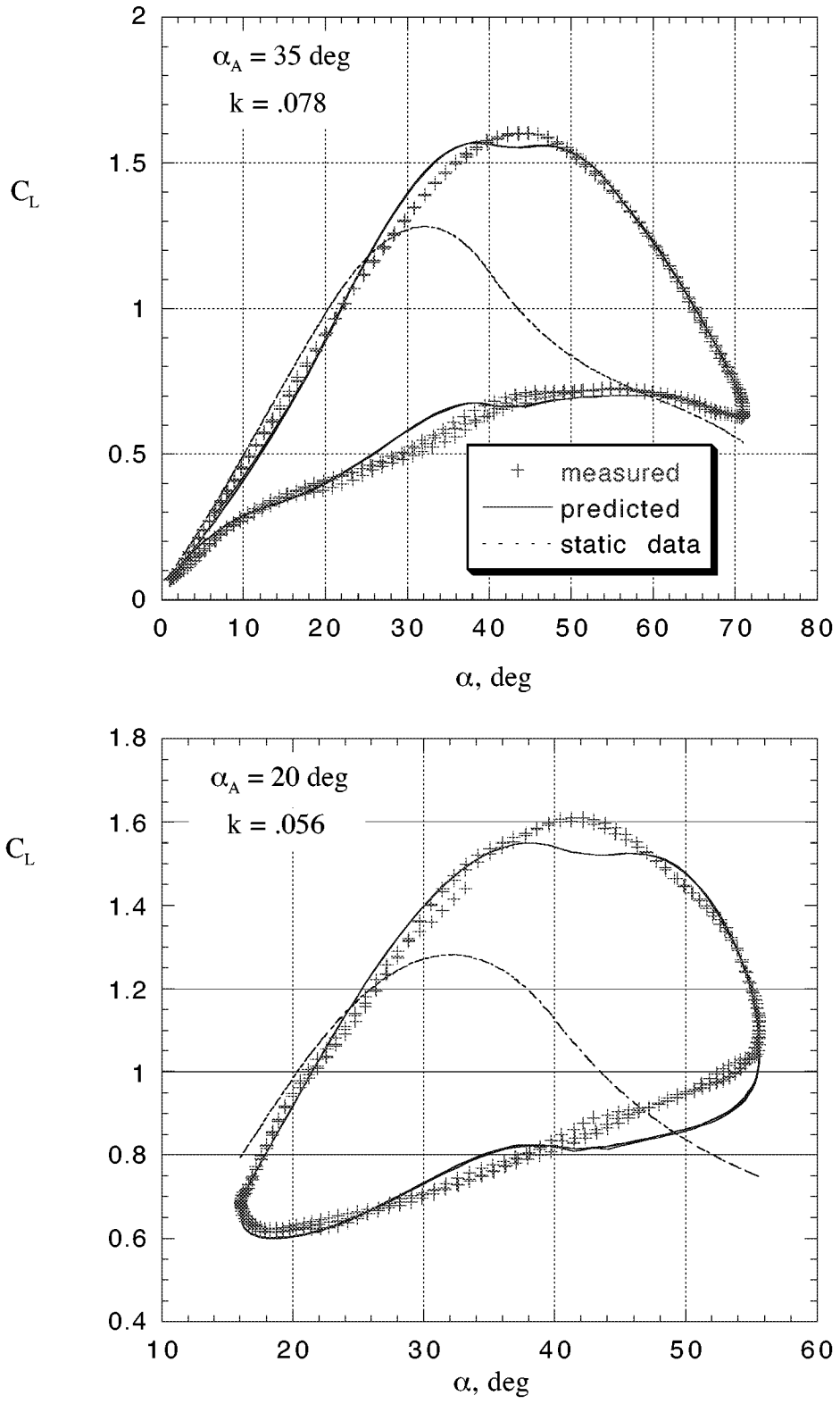

Figure 11. Measured and predicted lift coefficient at two amplitudes.

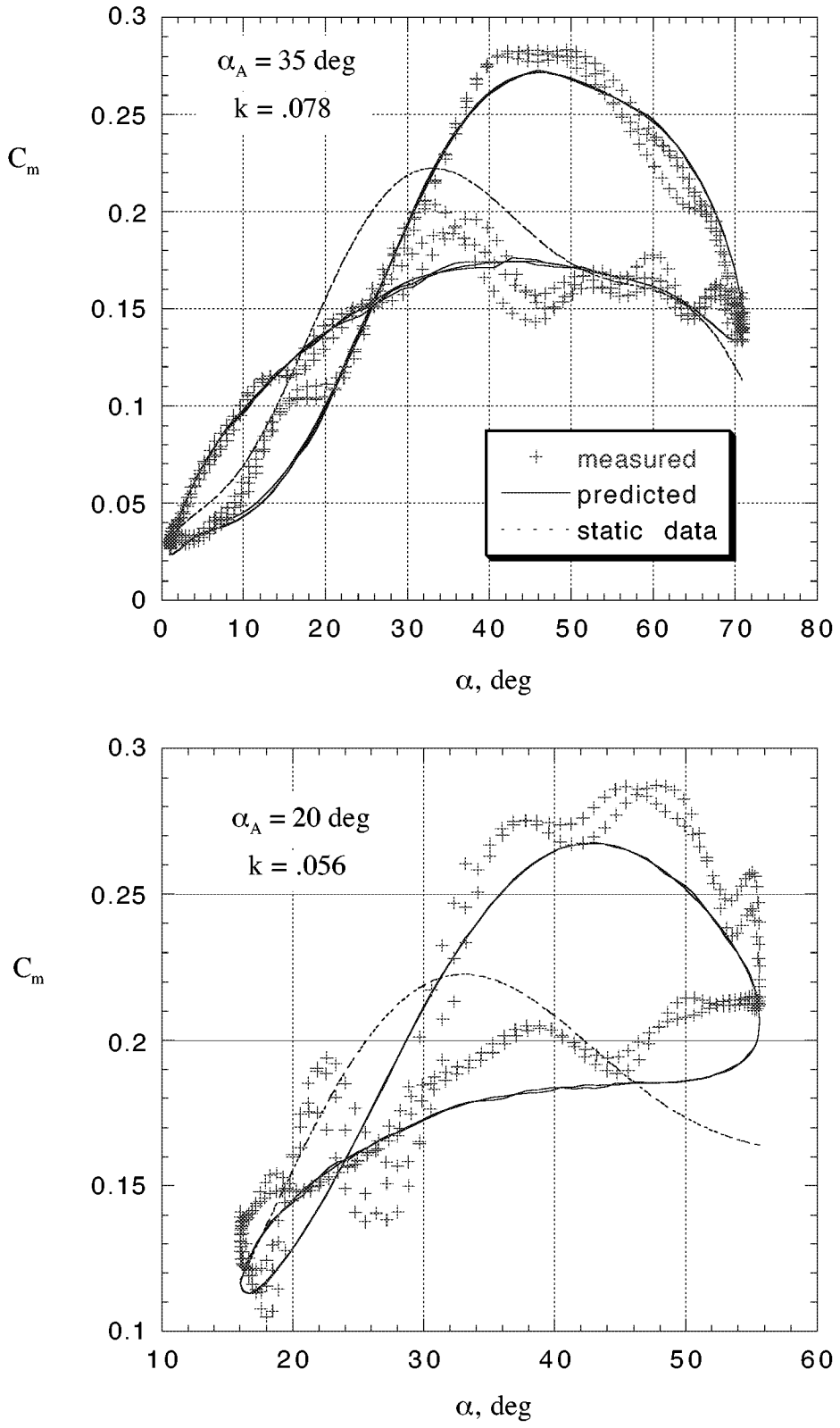

Figure 12. Measured and predicted pitching-moment coefficient at two amplitudes.

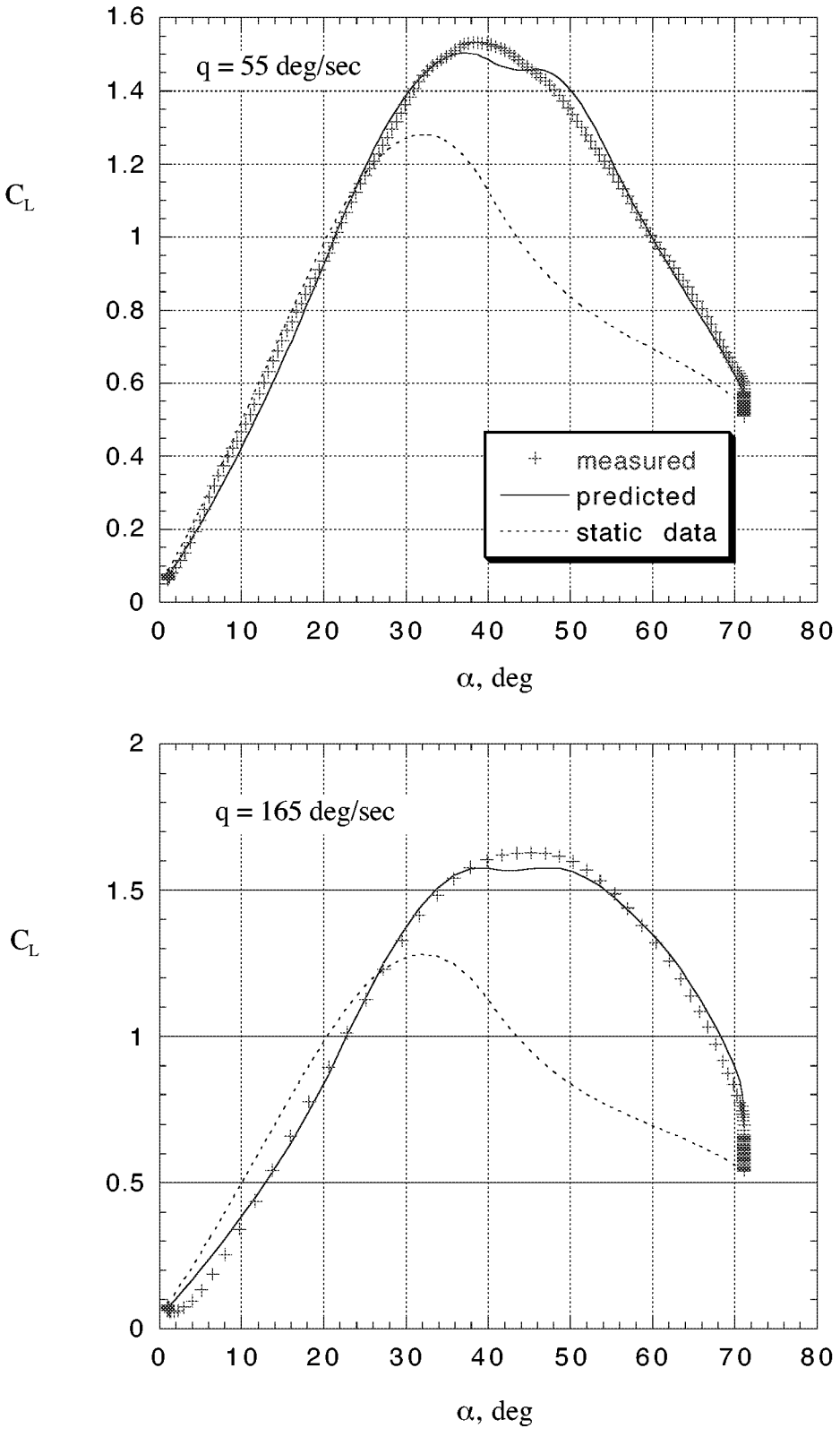

Figure 13. Measured and predicted lift coefficient at two input rates.

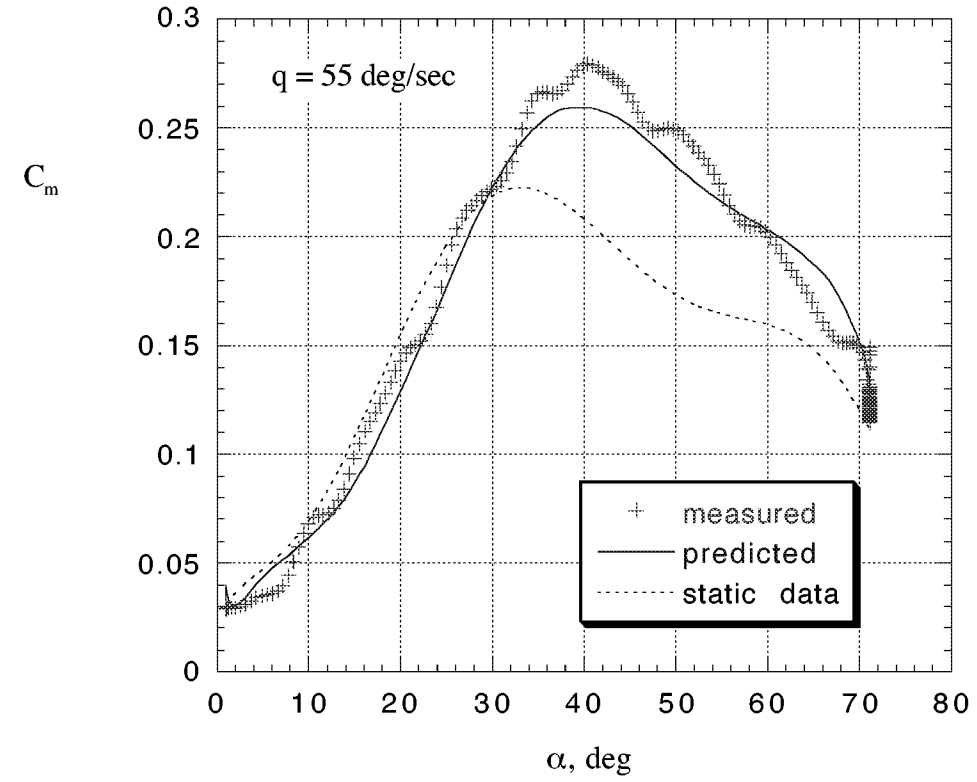

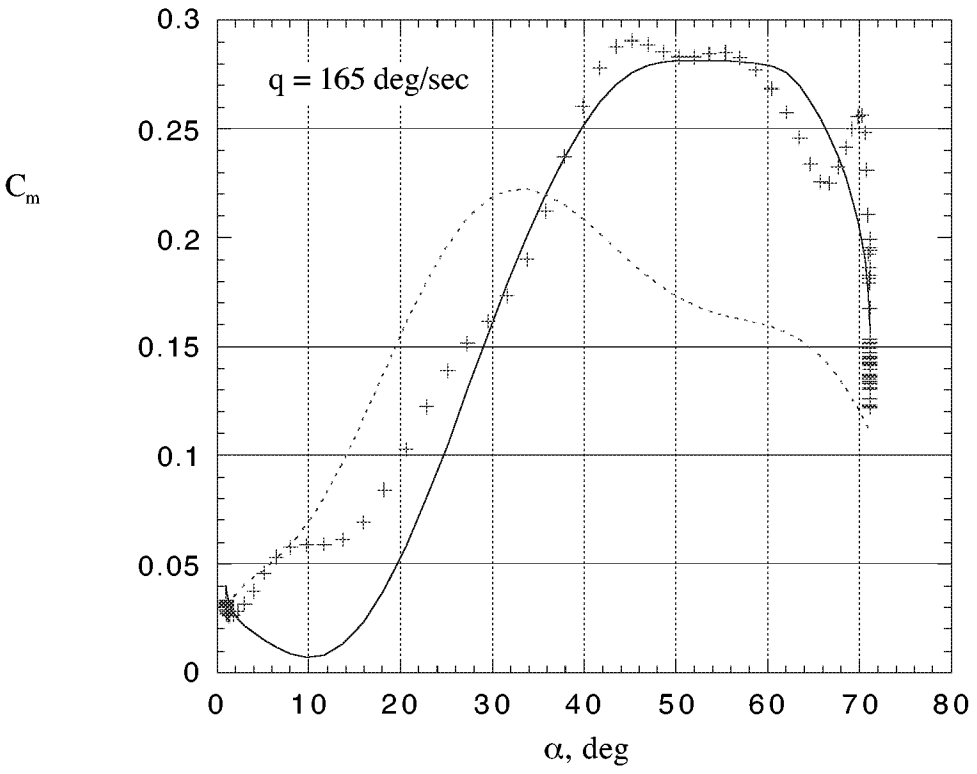

Figure 14. Measured and predicted pitching-moment coefficients at two rates.

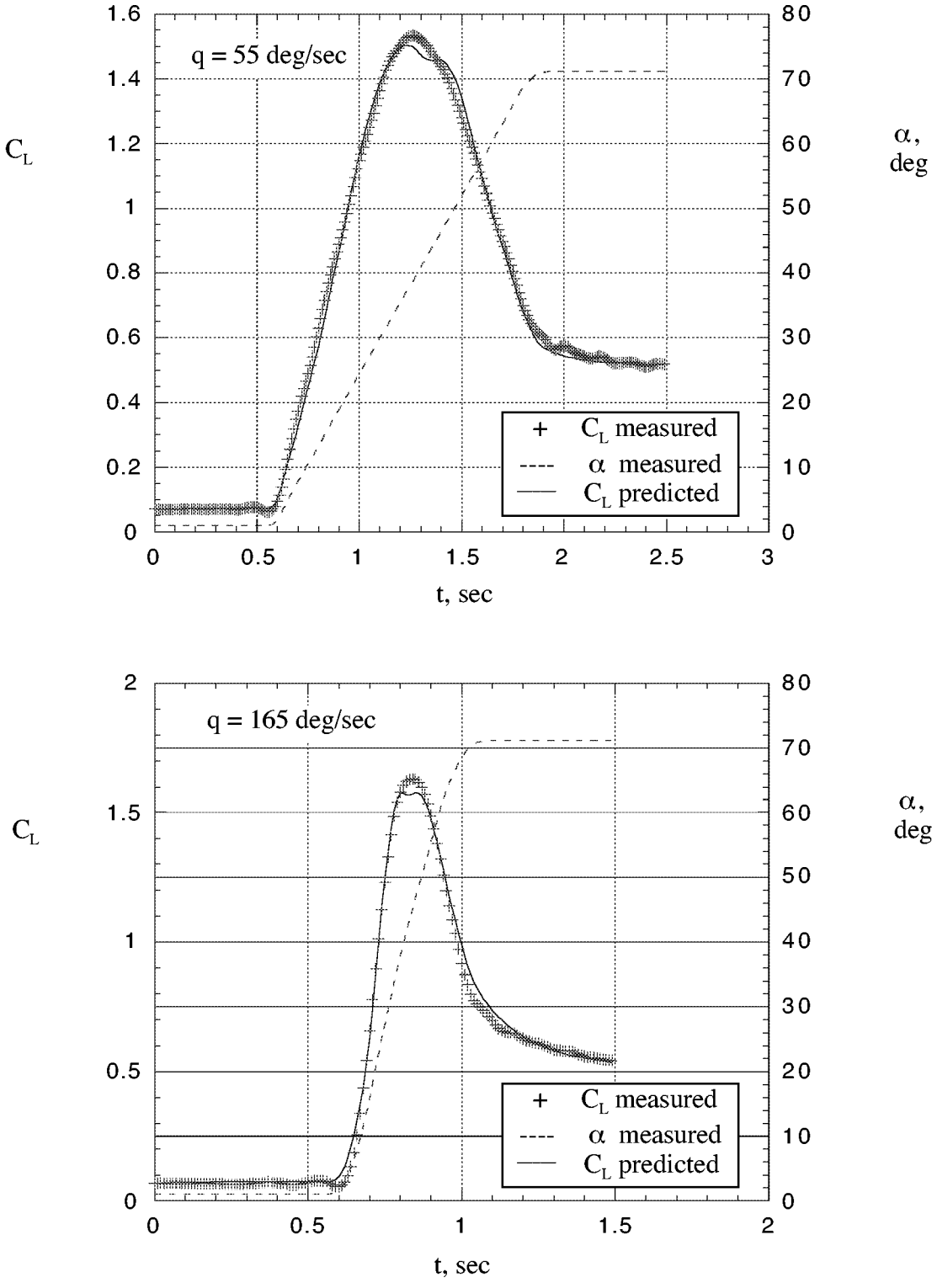

Figure 15. Time histories of angle of attack and lift coefficient at two input rates.

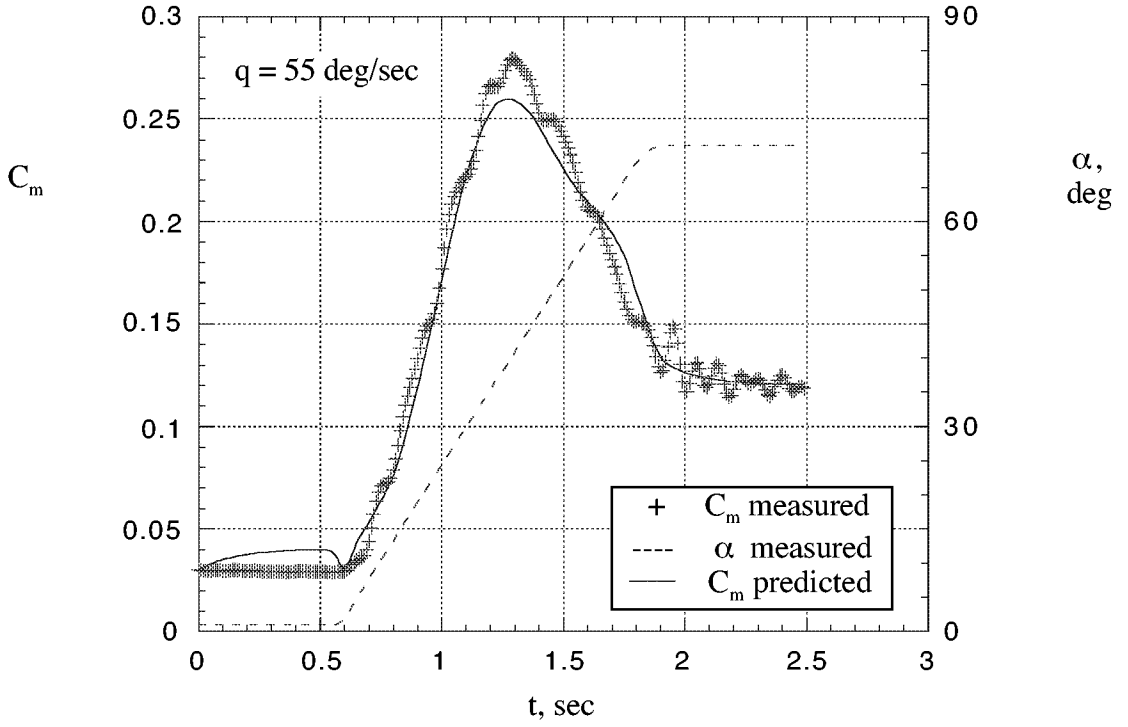

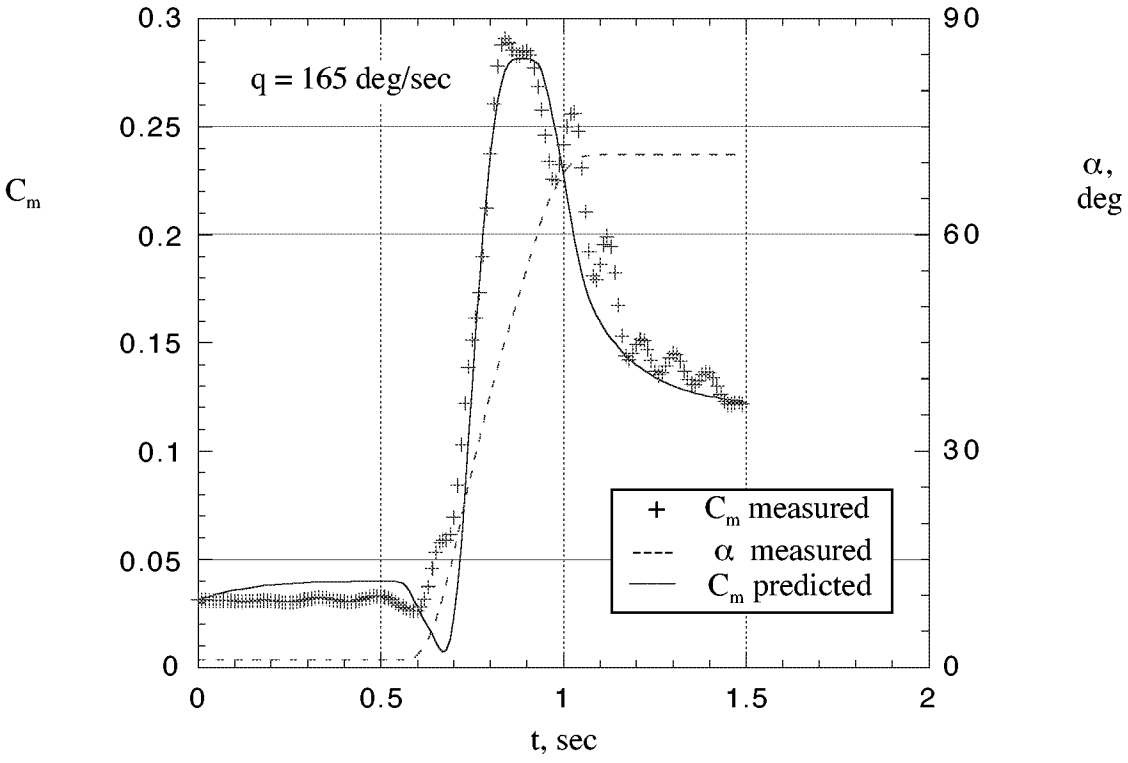

Figure 16. Time histories of angle of attack and pitching-moment coefficients at two rates.

REPORT DOCUMENTATION PAGE

Form Approved
OMB No. 0704-0188

1. AGENCY USE ONLY (*Leave blank*)	2. REPORT DATE	3. REPORT TYPE AND DATES COVERED
	December 1998	Technical Memorandom

4. TITLE AND SUBTITLE

Estimation of Aircraft Nonlinear Unsteady Parameters From Wind Tunnel Data

5. FUNDING NUMBERS

522-33-11-05

6. AUTHOR(S)

Vladislav Klein and Patrick C. Murphy

7. PERFORMING ORGANIZATION NAME(S) AND ADDRESS(ES)

NASA Langley Research Center
Hampton, VA 23681-2199

8. PERFORMING ORGANIZATION REPORT NUMBER

L-17805

9. SPONSORING/MONITORING AGENCY NAME(S) AND ADDRESS(ES)

National Aeronautics and Space Administration
Washington, DC 20546-0001

10. SPONSORING/MONITORING AGENCY REPORT NUMBER

NASA/TM-1998-208969

11. SUPPLEMENTARY NOTES

Klein: George Washington University, JIAFS, Langley Research Center, Hampton, Virginia
Murphy: NASA Langley Research Center, Hampton, Virginia

12a. DISTRIBUTION/AVAILABILITY STATEMENT

Unclassified-Unlimited
Subject Category 08 Distribution: Standard
Availability: NASA CASI (301) 621-0390

12b. DISTRIBUTION CODE

13. ABSTRACT *(Maximum 200 words)*

Aerodynamic equations were formulated for an aircraft in one-degree-of-freedom large amplitude motion about each of its body axes. The model formulation based on indicial functions separated the resulting aerodynamic forces and moments into static terms, purely rotary terms and unsteady terms. Model identification from exprimental data combined stepwise regression and maximum likelihood estimation in a two-stage optimization algorithm that can identify the unsteady term and rotary term if necessary. The identification scheme was applied to oscillatory data in two examples. The model identified from experimental data fit the data well, however, some parameters were estimated with limited accuracy. The resulting model was a good predictor for oscillatory and ramp input data.

14. SUBJECT TERMS

unsteady aerodynamics, indicial functions,
system identification, wind tunnel oscillatory data

15. NUMBER OF PAGES

43

16. PRICE CODE

A03

17. SECURITY CLASSIFICATION OF REPORT	18. SECURITY CLASSIFICATION OF THIS PAGE	19. SECURITY CLASSIFICATION OF ABSTRACT	20. LIMITATION OF ABSTRACT
Unclassified	Unclassified	Unclassified	